Electronic Supplementary Material (ESI) for Journal of Materials Chemistry A.

Interfacial Synergy of Ultralong Jagged $Pt_{85}Mo_{15}$-S Nanowires with Abundant Active Sites on Enhanced Hydrogen Evolution in Alkaline Solution

Yao Wang,[a,1] Hongying Zhuo,[a,b,1] Xin Zhang,[a,*] Yunrui Li,[a] Juntao Yang,[a] Yujie Liu,[a] Xiaoping Dai,[a] Mingxuan Li,[a] Huihui Zhao,[a] Meilin Cui,[a] Hai Wang,[c] Jun Li[b,*]

[a]State Key Laboratory of Heavy Oil Processing, College of Chemical Engineering, China University of Petroleum, Beijing 102249, China

[b]Department of Chemistry and Key Laboratory of Organic Optoelectronics & Molecular Engineering of Ministry of Education, Tsinghua University, Beijing 100084, China

[c]National Institute of Metrology, Beijing 100013, China

[1]These authors contributed equally to this work.

Corresponding author: Xin Zhang* E-mail: zhangxin@cup.edu.cn

Jun Li* E-mail: junli@mail.tsinghua.edu.cn

Chemicals: Chloroplatinic acid ($H_2PtCl_6.6H_2O$), potassium hydroxide (KOH), sodium sulphide (Na_2S) and sodium hydroxide (NaOH) were bought from Sinopharm Chemical Reagent Co., Ltd. Commercial Pt/C (20 weight percent (wt %) Pt on Vulcan XC72R carbon; Pt particle size, 2 to 5 nm) and molybdenum chloride ($MoCl_5$) were purchased from Alfa Aesar. N, N-dimethyl formamide (DMF), and ethanol were purchased from the Beijing Chemical Reagent Co., Ltd. ethylene glycol (EG) was purchased from Tianjin recovery chemical reagent Co., Ltd. All reagents were analysis reagent (A. R.), and used as received without further purification. Deionized water (Milli-Q) was used for the synthesis of nanomaterials.

Materials Characterization: Transmission electron microscopy (TEM) was carried out on JEM-2100 at 200 kV. The magnified images were observed on a Tecnai G2 F20 S-Twin high resolution transmission electron microscope (HRTEM) operating at 200 kV. X-ray diffraction (XRD) patterns were performed on a Brüker D8 advance diffractometer at 40 kV and 40 mA for Cu Kα (λ= 0.15406), with a scan speed of 5 ^{o}/min and a step size of 0.02 in 2θ. X-rayphotoelectron spectrum (XPS) analysis was measured on a PHI 5000 Versaprobe system using monochromatic Al Kα radiation (1486.6 eV), and all binding energies were calibrated by the C1s peak at 284.3 eV. Inductively coupled plasma-optical emission spectroscopy (ICP-OES) was performed on IRIS Intrepid II XSP (Thermo Fisher), Working parameters: RF power, 1150 W; nebulizer flow, 26.0 PSI; auxiliary gas, 1.0 LPM.

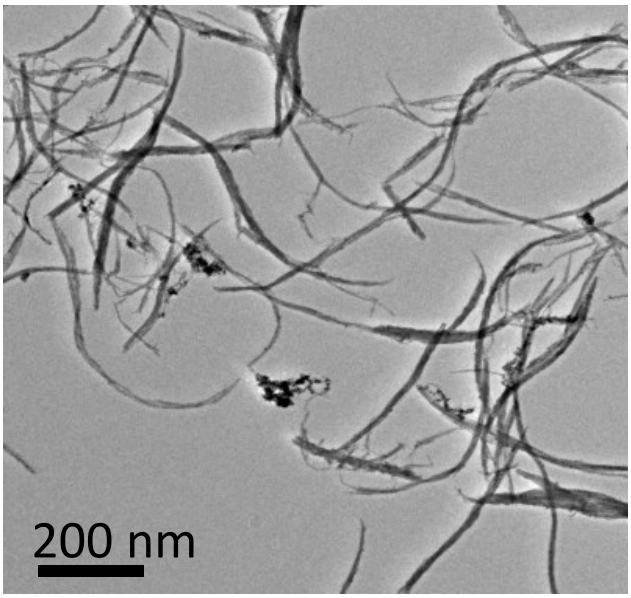

Fig. S1 TEM image of $Pt_{85}Mo_{15}$ NWs.

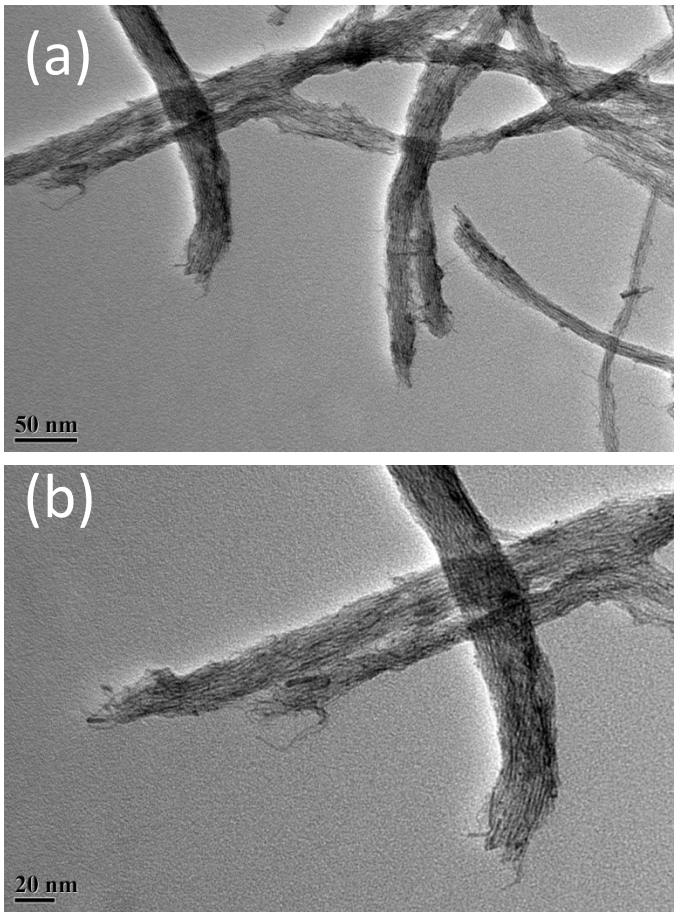

Fig. S2 (a, b) Enlarged TEM images of $Pt_{85}Mo_{15}$ NWs.

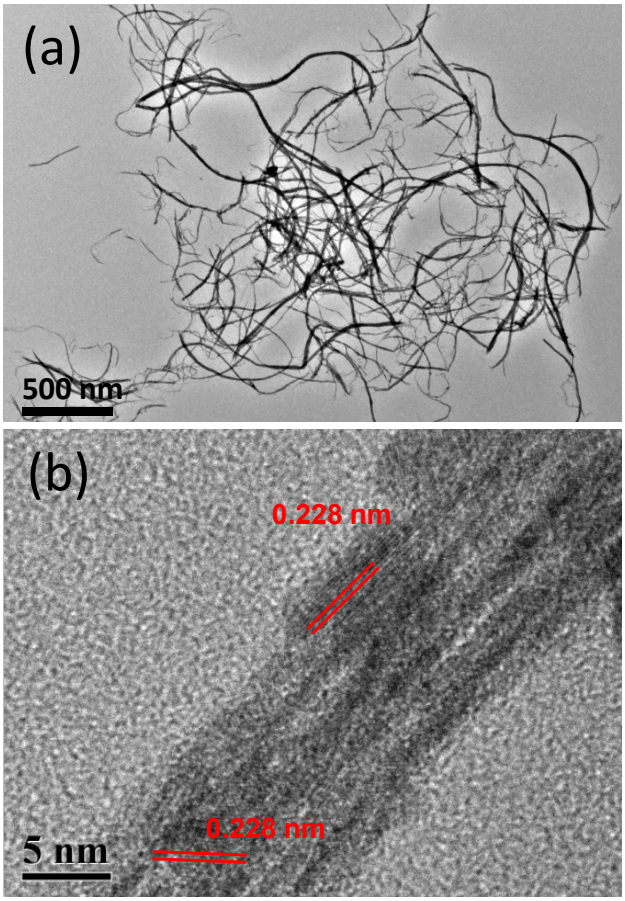

Fig. S3 (a) TEM image of Pt NWs, (B) enlarged TEM image of Pt NWs.

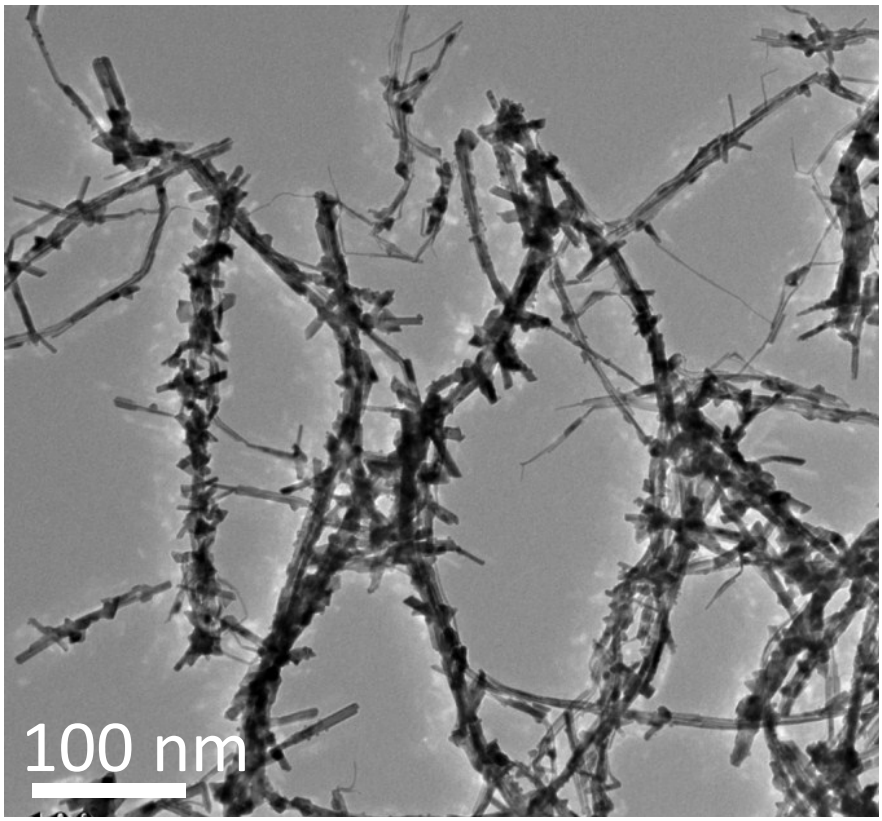

Fig. S4 TEM image of $Pt_{85}Mo_{15}$-S NWs.

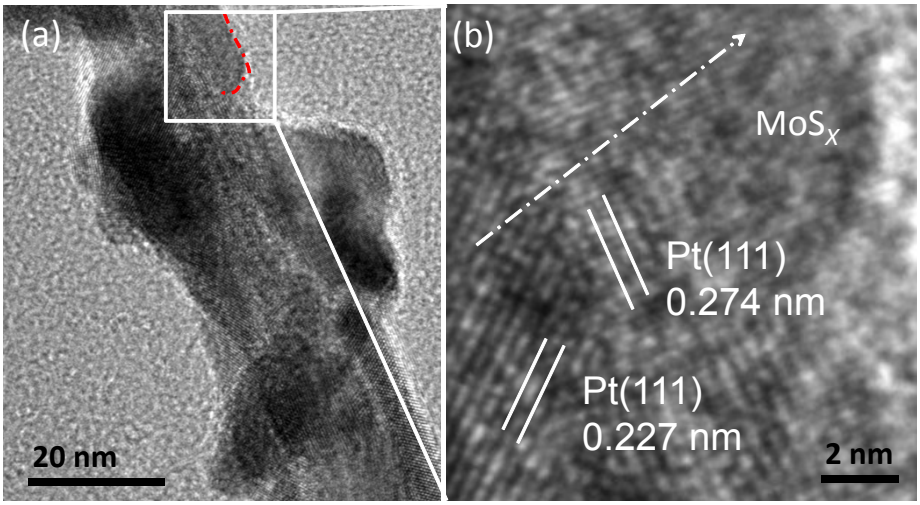

Fig. S5 (a, b) HRTEM images of PtMo-S NWs

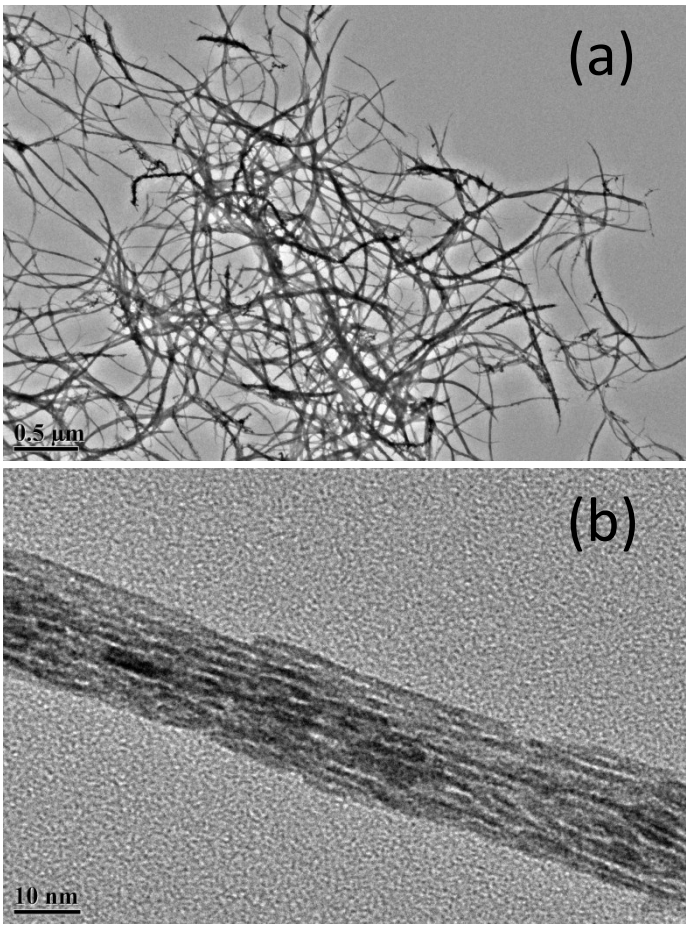

Fig. S6 (a,b) TEM images of Pt-S NWs.

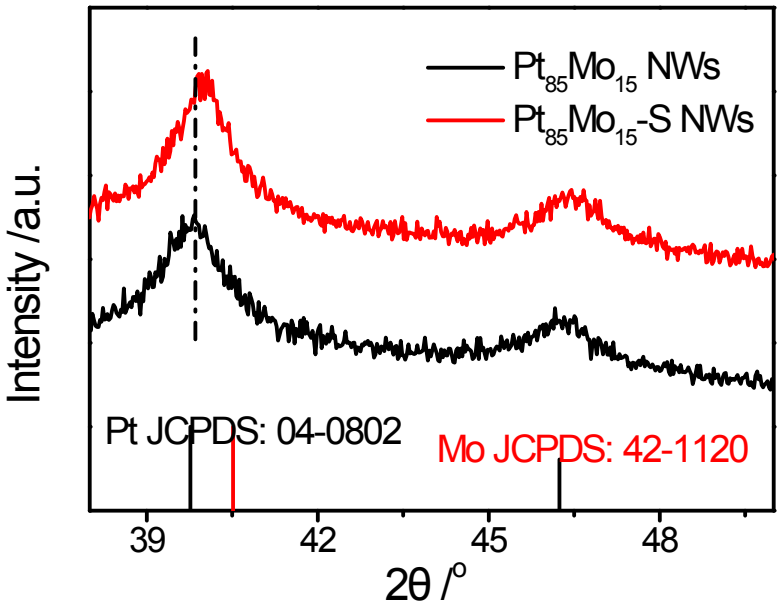

Fig. S7 Enlarged XRD patterns of $Pt_{85}Mo_{15}$ NWs and $Pt_{85}Mo_{15}$-S NWs.

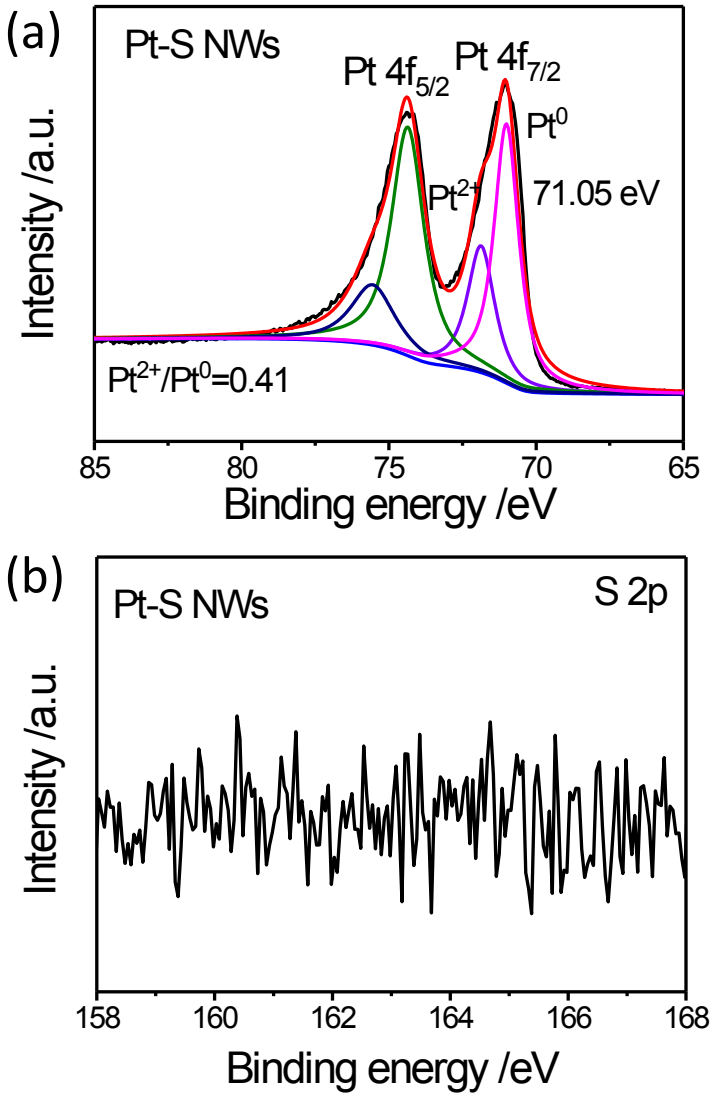

Fig. S8 (a) XPS patterns of the Pt 4f of Pt-S NWs, (b) XPS patterns of the S 2p of Pt-S NWs.

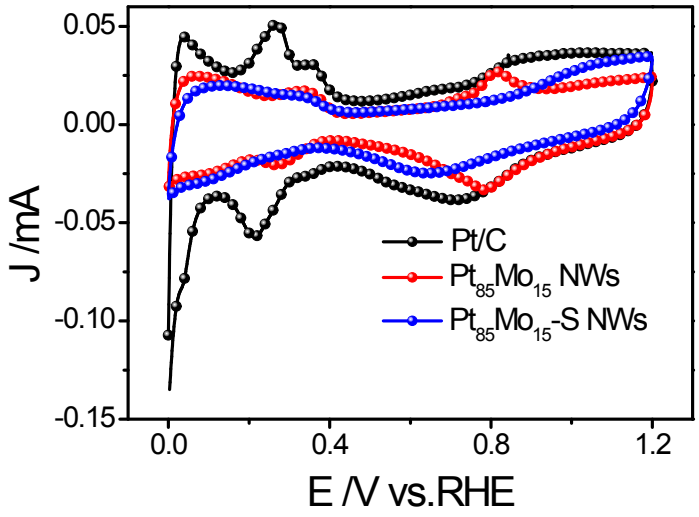

Fig. S9 Cyclic voltammetry curves of $Pt_{85}Mo_{15}$ NWs, $Pt_{85}Mo_{15}$-S NWs and Pt/C.

Note: H_{upd}-ECSA Evaluation: To evaluate the H_{upd} based ECSA the last cycle which was recorded with 50 mV s^{-1} before activity measurements was selected. The cyclic voltammetry was performed between 0 and 1.20 V vs. RHE with a scan rate of 50 mV s^{-1} under nitrogen atmosphere. The values were calculated integrating the cyclic voltammogram (CV) between 0 and 0.4 V. The measured Q_H value was normalized with respect to the theoretical value of Q_H^{theo} = 210 μC cm^{-2}, which is assuming a one electron transfer between one H atom and one Pt atom.

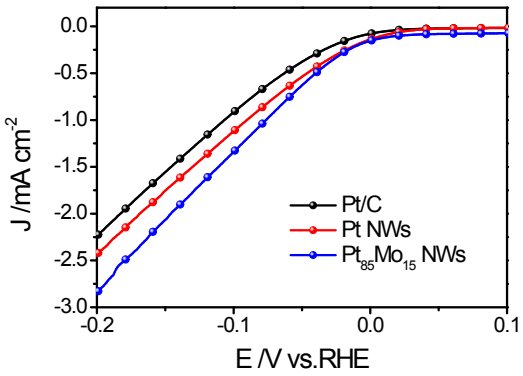

Fig. S10 HER activities of pure Pt NWs, $Pt_{85}Mo_{15}$-S NWs and commercial Pt/C.

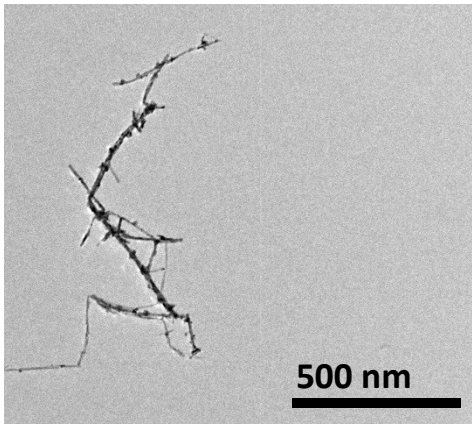

Fig. S11 TEM images of $Pt_{85}Mo_{15}$-S NWs after 3,000 potential cycles in 0.1 M NaOH solution.

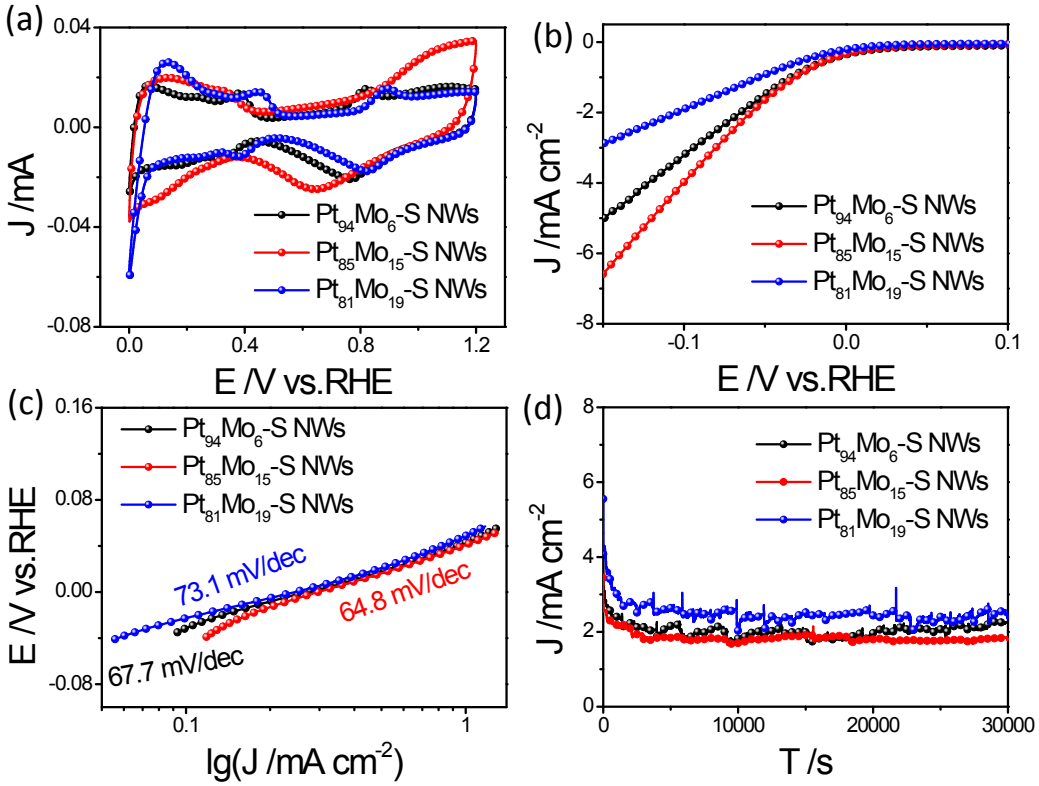

Fig. S12 (a) Cyclic voltammetry (CV) curves, (b) Linear sweep voltammetry (Lsv) curves, (c) Tafel plots of the polarization curves in b and (d) Chronoamperometry curves of $Pt_{94}Mo_6$-S, $Pt_{85}Mo_{15}$-S and $Pt_{81}Mo_{19}$-S NWs.

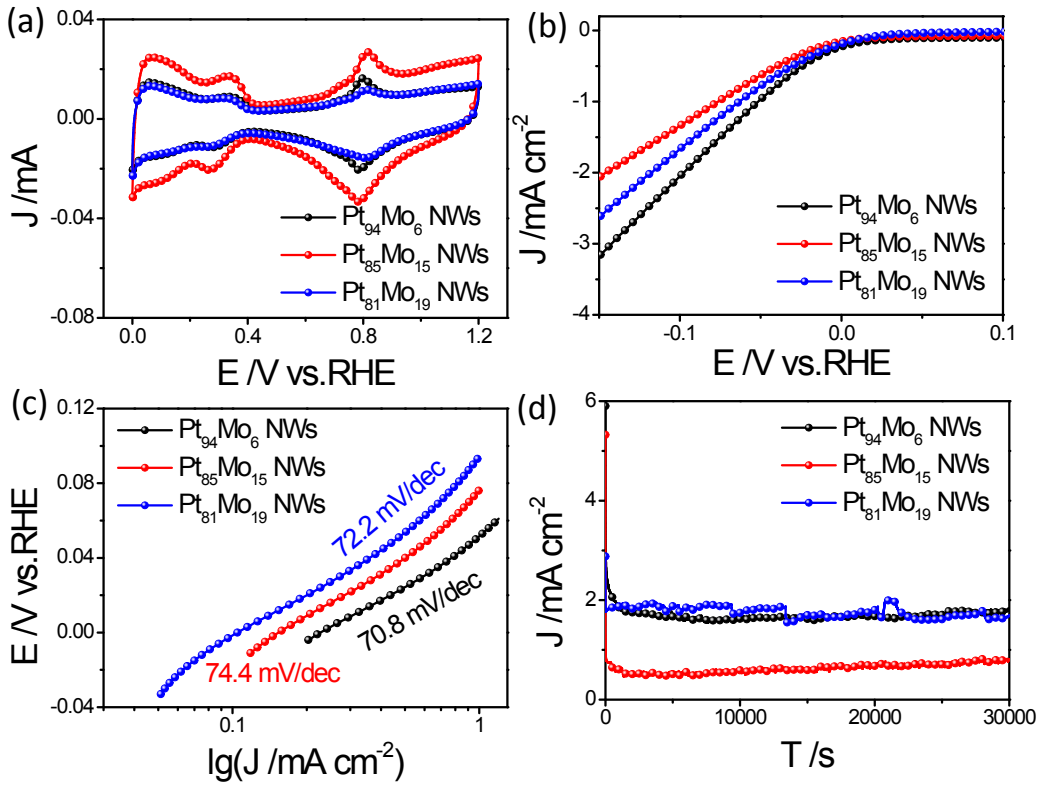

Fig. S13 (a) Cyclic voltammetry curves, (b) Linear sweep voltammetry (Lsv) curves, (c) Tafel plots of the polarization curves in b and (d) chronoamperometry of $Pt_{94}Mo_6$, $Pt_{85}Mo_{15}$ and $Pt_{81}Mo_{19}$ NWs.

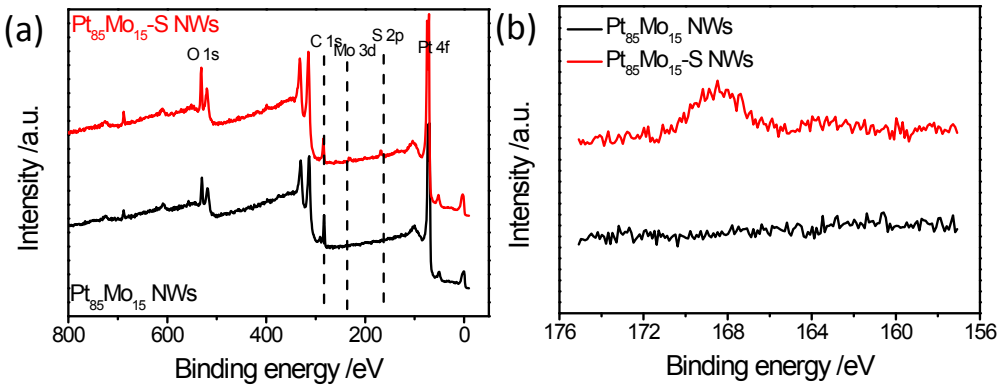

Fig. 14 (a) Elemental spectra regions of XPS spectra of the as-prepared $Pt_{85}Mo_{15}$ and $Pt_{85}Mo_{15}$-S NWs after the stability tests. (b) XPS patterns of the S 2p of the as-prepared $Pt_{85}Mo_{15}$ and $Pt_{85}Mo_{15}$-S NWs.

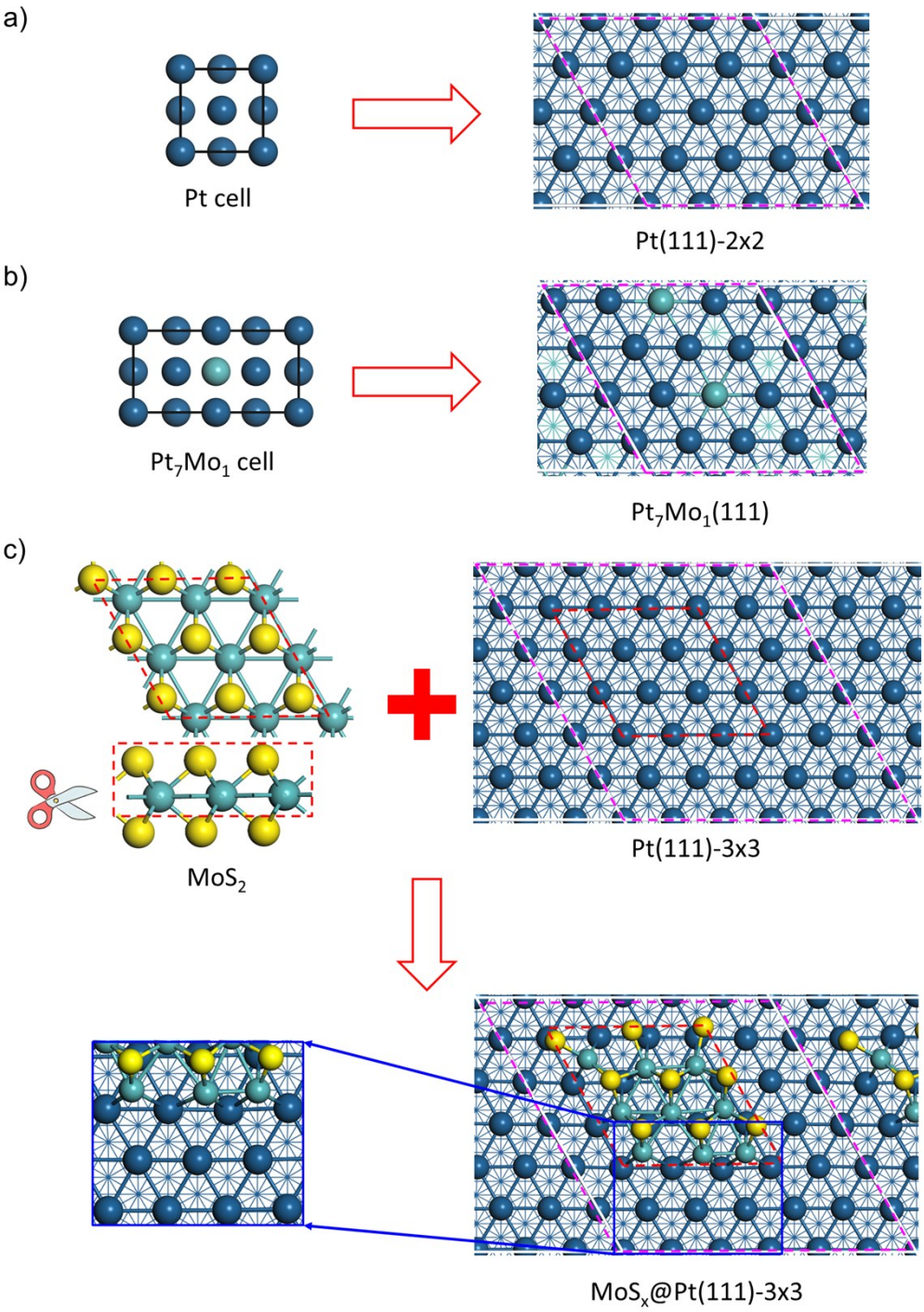

Fig. S15 Models of (a) Pt(111), (b) $Pt_7Mo_1(111)$, (c) MoS_x@Pt(111).

Note: The Pt(111) and $Pt_7Mo_1(111)$ surface were modeled by periodically repeated four-layer slabs with (2x2) unit cells. The atoms in the top two layers were fully relaxed, while the rest of the atoms were fixed in their equilibrium positions. For the MoS_x@Pt(111) surface, Pt(111) with (3x3) unit cells was used as the substrates, in order to avoid the interactions of supported MoS_x cluster between adjacent units.

Table S1. The compositions of Pt: Mo in all catalysts determined by ICP-OES.

Catalysts	Molar ratio (Pt: Mo)
$Pt_{94}Mo_6$ NWs	94: 6
$Pt_{85}Mo_{15}$ NWs	85: 15
$Pt_{81}Mo_{19}$ NWs	81: 19
$Pt_{94}Mo_6$-S NWs	91: 9
$Pt_{85}Mo_{15}$-S NWs	79: 21
$Pt_{81}Mo_{19}$-S NWs	73: 27